PHYSICAL REVIEW B VOLUME 29, NUMBER 2 15 JANUARY 1984

Theoretical study of O chemisorption on NiO. Perfect surfaces and cation vacancies

J. M. Blaisdell* and A. B. Kunz
Department of Physics and Materials Research Laboratory, University of Illinois at Urbana—Champaign, Urbana, Illinois 61801
(Received 6 June 1983)

Self-consistent unrestricted Hartree-Fock calculations are presented for the adsorption of atomic oxygen onto the nickel oxide (100) surface. The perfect surface is shown to be nonreactive, but enhanced binding is found for vacancy sites in the first two atomic layers. Of particular interest is a second-layer anion-vacancy site. Various charge states are examined and charge transfer between adsorbate and surface are noted. A calculation for molecular oxygen in the neighborhood of a second-layer anion vacancy is also presented. O_2 is found to bind to the surface less strongly than atomic oxygen, and accordingly a dissociation site is postulated. Analysis of the character of the electrons on the transition-metal atom indicates that bonding is localized in the *s*- and *p*-character electrons rather than in the *d* electrons.

I. INTRODUCTION

Previous studies[1,2] have examined the adsorption of hydrogen on the surface of NiO using a cluster model of the (100) surface which describes the electronic structure of the surface successfully.[3] It was determined that the perfect surface is almost inert in this reaction, but that defects in the first and second layers provide a variety of active sites for hydrogen chemisorption. In the present work, calculations are extended to the physically interesting case of oxygen adsorption on the perfect NiO(100) surface and selected defects. Several possible sites are investigated by *ab initio* methods to determine the potentials near them. Calculations for both atomic O and molecular O_2 are reported.

Adsorption of O_2 and CO and NiO was studied extensively by Gravelle and Teichner,[4] who determined that although large initial heats of adsorption are found (60—114 kcal/mol) the maximum surface coverage is only a few percent of the first atomic layer. Iwamoto *et al.*[5] have confirmed this result and have recognized that several different adsorption sites are active with a maximum coverage of 4%.

The limited coverage observed suggests that defect sites are active in the oxygen adsorption. A series of radiation damage studies by Charman and Dell[6] discovered that the number of radiation-induced displacements in the lattice corresponded roughly to the increased amount of oxygen which was taken up by the lattice. The exact sites of adsorption were not determined.

Wagner and Hauffe[7] studied the catalytic oxidation of CO as well as the catalytic decomposition of N_2O and concluded that "adsorbed O" was the intermediate in both reactions. Other studies have indicated that catalytic activity is increased if excess oxygen is preadsorbed on the surface,[8,9] establishing that adsorbed oxygen plays an important role in the catalysis. It is clear that an understanding of the oxygen adsorption on the nickel oxide surface is basic to an appreciation of the catalytic reactions which take place on the surface.

The intrinsic defect structure of the NiO has been investigated by a number of authors. Lesage *et al.*[10] measured the diffusion of nickel ions through NiO and concluded that the predominant defect was a nickel vacancy with two electrons localized on the site having a concentration of 10^{-7}. Koel and Gellings[11] have proposed that neutral, singly ionized, and doubly ionized vacancies on both cationic and anionic sublattices are present in significant number, with the major species being a nickel vacancy with one electron in a concentration of 10^{-5}. Shirasaki *et al.*[12] have presented some evidence that oxygen vacancies may be plentiful under some circumstances. They are able to vary greatly the oxygen diffusion rate by doping with alumina. In light of work by Atkinson and Taylor,[13] who report that diffusion studies of tracer nickel show greatly enhanced diffusion near grain boundaries, thus that defect concentrations are likely higher near the surface than in the bulk, all vacancy species must be considered as candidates for the adsorption site.

Section II will discuss the cluster model and methods used. Section III will discuss calculational results for the perfect surface, some of which were reported in preliminary form earlier,[14] followed by results for the defective surfaces. Further discussion and conclusions will be found in Sec. IV.

II. CLUSTER MODELS

As in work reported previously, we employ small clusters of Ni and O ions embedded in a point-ion field as a model for the solid surface. The point-ion array is a $5\times5\times4$ matrix (charge ±2) that provides charge neutrality and the correct Madelung potential for the clusters. The cluster is illustrated in Fig. 1 for the case of an oxygen atom above an Ni site on the perfect surface. As shown in Fig. 1, the surface cluster proper consists of a quincunx of ions in the first layer and one ion from the second layer. Simple modifications are made to form the other clusters. All of the results reported here were ob-

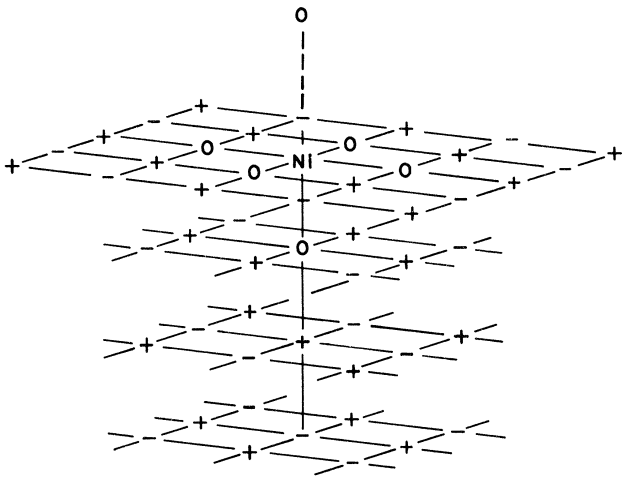

FIG. 1. Model of the adsorption site showing atoms on which basis functions are centered, as well as the point-ion array. Lower three levels are also 5×5 in the calculation but the outer rows have been omitted for clarity.

tained from self-consistent unrestricted Hartree-Fock calculations.[3]

For the case of a second-layer anion vacancy, the O atom is removed from the backing position in the cluster, leaving behind two electrons. For the first-layer anion vacancy, the nickel and oxygen sublattices are reversed and the O is removed from the central position in the surface layer. The only position of the O_2 molecule considered to date locates the second oxygen atom directly above the one shown in the adsorption in Fig. 1.

The calculations presented in this work have all involved the (100) surface as it might be found after cleaving. It has been assumed that there is no reconstruction of the surface. Support from this view comes from work of Prutton *et al.*[15] They report from low-energy electron diffraction (LEED) data that the termination of the bulk lattice is indeed the simple (100) face, with an upper limit for dimensional modification of 2% of the interatomic spacing for any surface reconstruction.

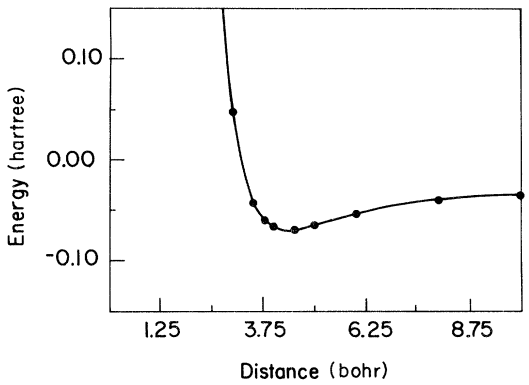

FIG. 3. Binding curve for O^- above the perfect surface has a minimum of −0.069 hartree at 4.4 bohrs.

III. RESULTS AND DISCUSSION

The most advantageous location for binding on the perfect surface is likely to be on top of a nickel ion, which is the position chosen for the model. The distance of the oxygen was varied from 3 to 10 bohrs, which latter distance resembles the infinite separation case.

The potential for neutral oxygen is shown in Fig. 2. The minimum value for this curve is 5.1 bohr, just greater than the lattice spacing. The depth of the potential well is only 0.011 hartree (0.3 eV), however, and this binding is not strong compared to the values observed in the experiments discussed above.

Potential curves were also calculated for possible adsorption of the free ions O^- and O^{2-}. These curves are shown in Figs. 3 and 4. The minima of the wells are found to be −0.069 and −0.110 hartree, or −1.9 and −3.0 eV, respectively, at distances near 4.5 bohr. These binding energies are strong enough to indicate that reaction intermediates with negatively charged oxygen at one end may bind to the perfect surface in catalyzed reactions. However, for O_2 to dissociate and bind, more energy must be found; the dissociation energy of O_2 is 5.2 eV. For a molecule to dissociate and bind as two double ionized atoms yields a gain of only 0.4 eV per atom, not nearly the

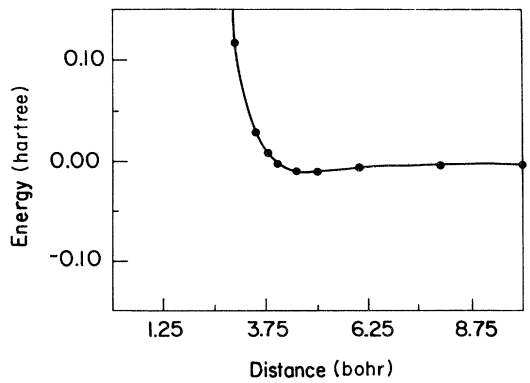

FIG. 2. Binding curve for neutral O above the perfect surface has a minimum of −0.011 hartree at 5.1 bohrs.

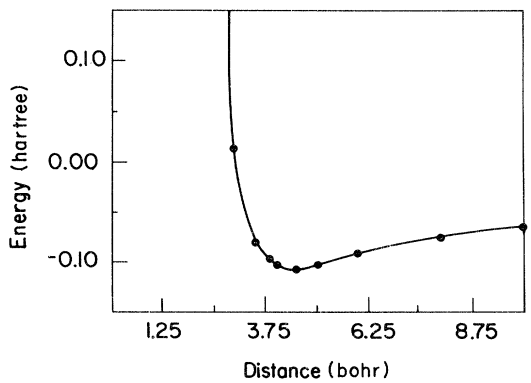

FIG. 4. Binding curve for O^{2-} above the perfect surface has a minimum of −0.109 hartree at 4.4 bohrs.

TABLE I. O above Ni on perfect surface.

Distance	Energy	Mulliken populations			
		Adsorbed O	Surface Ni	Surface O[a]	Second-layer O
∞	0.0000	8.0000	8.2257	7.9546	7.9560
10	−0.0043	7.9975	8.2284	7.9546	7.9555
8	−0.0056	7.9876	8.2379	7.9549	7.9550
6	−0.0075	7.9643	8.2529	7.9568	7.9558
5	−0.0110	7.9562	8.2527	7.9590	7.9551
4.5	−0.0099	7.9625	8.2494	7.9586	7.9536
4	−0.0012	7.9854	8.2377	7.9563	7.9517
3.8	+0.0070	8.0022	8.2297	7.9544	7.9504
3.5	+0.0269	8.0389	8.2120	7.9501	7.9486
3	+0.1159	8.1184	8.1877	7.9376	7.9435

Distance	Populations on surface Ni by character		
	s	*p*	*d*
∞	0.0564	0.1578	8.0116
10	0.0564	0.1606	8.0114
8	0.0581	0.1686	8.0112
6	0.0694	0.1712	8.0123
5	0.0769	0.1608	8.0148
4.5	0.0804	0.1522	8.0168
4	0.0833	0.1366	8.0177
3.8	0.0842	0.1288	8.0167
3.5	0.0877	0.1137	8.0108
3	0.1128	0.1023	7.9726

[a]Average value; there is a slight variation.

TABLE II. O^- above Ni on perfect surface.

Distance	Energy	Mulliken populations			
		Adsorbed O	Surface Ni	Surface O[a]	Second-layer O
∞	0.0000	9.0000	8.2257	7.9546	7.9560
10	−0.0335	8.9970	8.2013	7.9597	7.9629
8	−0.0396	8.9839	8.1983	7.9632	7.9651
6	−0.0527	8.9394	8.2044	7.9714	7.9704
5	−0.0638	8.9075	8.2118	7.9770	7.9727
4.5	−0.0688	8.8983	8.2127	7.9789	7.9734
4	−0.0667	8.9037	8.2051	7.9792	7.9741
3.8	−0.0610	8.9118	8.1991	7.9788	7.9740
3.5	−0.0437	8.9309	8.1868	7.9769	7.9746
3	+0.496	8.9498	8.1949	7.9700	7.9755

Distance	Populations on surface Ni by character		
	s	*p*	*d*
∞	0.0564	0.1578	8.0116
10	0.0471	0.1423	8.0119
8	0.0434	0.1428	8.0121
6	0.0483	0.1432	8.0131
5	0.0588	0.1378	8.0152
4.5	0.0650	0.1303	8.0173
4	0.0708	0.1139	8.0204
3.8	0.0722	0.1051	8.0217
3.5	0.0755	0.0875	8.0237
3	0.1002	0.0715	8.0231

[a]Average value; there is a slight variation.

TABLE III. O^{2-} above Ni on perfect surface.

Distance	Energy	Mulliken populations			
		Adsorbed O	Surface Ni	Surface O[a]	Second-layer O
∞	0.0000	10.0000	8.2257	7.9546	7.9560
10	−0.0649	9.9792	8.1972	7.9634	7.9698
8	−0.0761	9.9511	8.2033	7.9678	7.9742
6	−0.0924	9.9012	8.2120	7.9762	7.9819
5	−0.1039	9.8626	8.2254	7.9815	7.9860
4.5	−0.1092	9.8467	8.2330	7.9832	7.9876
4	−0.1068	9.8422	8.2357	7.9832	7.9894
3.8	−0.1007	9.8463	8.2348	7.9823	7.9897
3.5	−0.0822	9.8595	8.2311	7.9796	7.9908
3	+0.0129	9.8724	8.2547	7.9701	7.9925

Distance	Populations on surface Ni by character		
	s	*p*	*d*
∞	0.0564	0.1578	8.0116
10	0.0423	0.1426	8.0122
8	0.0388	0.1524	8.0121
6	0.0442	0.1554	8.0123
5	0.0582	0.1534	8.0138
4.5	0.0672	0.1505	8.0153
4	0.0760	0.1417	8.0181
3.8	0.0780	0.1372	8.0195
3.5	0.0818	0.1269	8.0224
3	0.1057	0.1220	8.0270

[a]Average value; there is a slight variation.

1—2 eV observed for the strong binding. This ionic state is not well localized; as can be seen from the curves, the trough is quite broad, extending quite far from the surface. It can be concluded that these cases are also unlikely candidates for the observed binding.

The small binding energy for the neutral case is analogous to the results found by Surratt and Kunz[1] for the simpler case of hydrogen adsorption on NiO. The binding energy of a hydrogen atom was found to be only 0.14 eV above a nickel site and 0.57 eV above an oxygen site. This confirms the finding of a relatively inert perfect surface. They reported a greatly enhanced binding of about 5 eV for a surface nickel vacancy and nearly 7 eV for a vacancy located on a crystallite corner.

Close examination of Tables I—III reveals the electron distribution among the atoms changes very little with the distance of the oxygen atoms from the surface. In all three cases there is a slight charge transfer from the adsorbed oxygen to the surface cluster, but this activity is not enough to form any strong bonds such as will be seen below. There is only a slight redistribution of charge among the surface atoms. Note particularly that although the population of the nickel site varies somewhat, the number of *d* electrons remains almost constant, with less

TABLE IV. O above neutral anion vacancy V_0.

Spin	Distance	Energy	Mulliken populations		
			Adsorbed O	Surface Ni[a]	Second-layer Ni
6 or 4	∞	0.0000	8.0000	8.4002	8.3994
6	10	+0.0002	8.0073	8.3991	8.3962
4	10	+0.0002	8.0073	8.3991	8.3962
6	6	−0.0018	8.1342	8.3699	8.3862
4	6	−0.0015	8.1295	8.3710	8.3864
6	3	−0.0563	8.8529	8.1706	8.4648
4	3	−0.0447	8.8600	8.1698	8.4607
6	1	−0.037	8.8094	8.1750	8.4906
5	1	−0.2378	9.5987	8.0782	8.0885
5	0	−0.27	10.0344	7.9843	8.0285

[a]Average value; there is a slight variation.

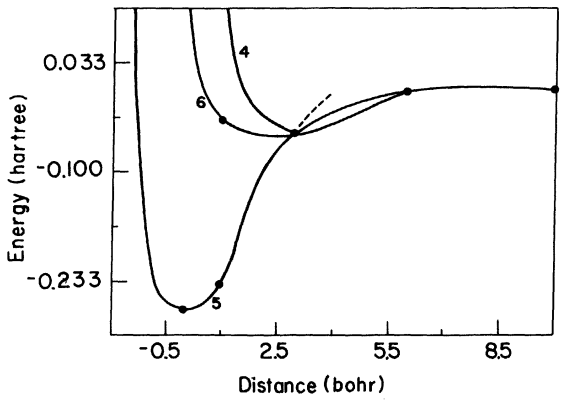

FIG. 5. Binding curve for O above an anion vacancy. Numbers on the figure indicate the spin of the state in question.

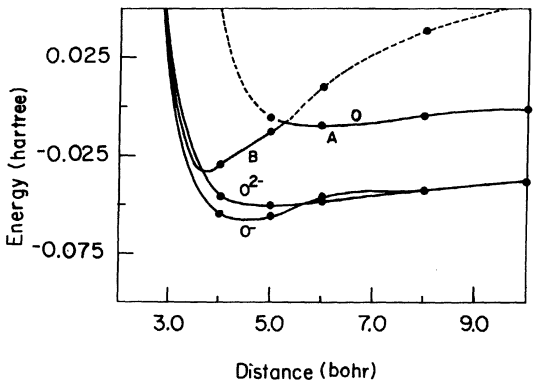

FIG. 6. Binding curves for O, O^-, and O^{2-} above a second-layer anion vacancy. The different electronic configurations are described in the text.

than $\frac{1}{100}$ of an elementary charge transferring until the oxygen collides with the nickel ion at around 3 bohr separation. The three potentials are all strongly repulsive in this region because of this collision. Changes in the *s*- and *p*-character properties are about an order of magnitude larger than the *d*-character change, and the variation, small though it is, is particularly rapid near the minima of the potential curves.

The ground state configuration for the surface alone is a triplet state, corresponding to saturated oxygen ions and the $3d^8$ state of nickel. In combination with the closed shell O^{2-}, the ground state remains a triplet. The spin increases to a quartet state with the O^- adsorption case and to a quintet for the neutral O case. Numerous other configurations were investigated briefly but these states as enumerated were confirmed to have the lowest energy.

It is natural that an oxygen atom binds strongly in a surface anion vacancy. There are a number of features of interest, however, in the data presented in Table IV and Fig. 5. The potential is of shorter range than the others in this study, and there are a number of spin states to be examined. One may as well regard this as the desorption potential for oxygen from a perfect surface.

The ground state of the Ni_5^{8+} cluster is, as reported by

TABLE V. O above Ni above second-layer vacancy.

Type	Distance	Energy	Vacancy	Mulliken populations Surface O	Surface Ni	Adsorbed O
A	∞	0.000 00	0.9113	7.9614	9.2433	8.0
A	10	−0.000 94	0.9093	7.9612	9.2486	7.9972
A	8	−0.005 84	0.8931	7.9612	9.2589	8.0030
B	8	+ 0.040 25	0.6431	7.9350	8.6394	8.9773
A	6	−0.010 00	0.8721	7.9608	9.2601	8.0245
B	6	+ 0.009 88	0.6563	7.9424	8.6604	8.9139
B	5	−0.013 06	0.6620	7.9476	8.6904	8.8575
A	5	−0.006 72	0.8690	7.9601	9.2571	8.0333
B	4	−0.030 39	0.6575	7.9499	8.7394	8.8035
B	3	+ 0.068 08	0.6484	7.9418	8.8525	8.7318

Type	Distance	Populations on surface Ni by character *s*	*p*	*d*
A	∞	0.4586	0.7670	8.0167
A	10	0.4635	0.7681	8.0169
A	8	0.4660	0.7757	8.0174
B	8	0.2134	0.4189	8.0071
A	6	0.4541	0.7894	8.0166
B	6	0.2211	0.4316	8.0076
B	5	0.2377	0.4423	8.0105
A	5	0.4680	0.7680	8.0212
B	4	0.2515	0.4691	8.0189
B	3	0.2759	0.5382	8.0384

TABLE VI. O^- above Ni above second-layer vacancy.

Type	Distance	Energy	Vacancy	Mulliken populations Surface O	Surface Ni	Adsorbed O
A	∞	0.000 00	0.9113	7.9614	9.2433	9.0000
A	10	−0.037 69	0.9486	7.9659	9.1910	8.9969
A	8	−0.042 19	0.9468	7.9689	9.1834	8.9942
A	6	−0.046 53	0.9537	7.9747	9.1632	8.9843
A	5	−0.056 17	0.9714	7.9807	9.1675	8.9377
A	4	−0.055 88	0.9645	7.9812	9.2133	8.8934
B?	3	+ 0.061 80	0.9425	7.9683	9.3374	8.8397

		Populations on surface Ni by character		
Type	Distance	*s*	*p*	*d*
A	∞	0.4586	0.7679	8.0167
A	10	0.4635	0.7681	8.0186
A	8	0.4446	0.7198	8.0189
A	6	0.4245	0.7202	8.0185
A	4	0.3973	0.7935	8.0226
B?	3	0.3971	0.9349	8.0054

Wepfer *et al.*[2] the state with spin 5. This is a reflection of the antiferromagnetic nature of the solid. The addition of the spin-1 oxygen at large distance forms either a state of spin 6 or a state of spin 4. Close by, the ground state is the state of spin 5, with the oxygen saturated and all the nickels aligned. This configuration becomes the lowest energy state around a distance above the surface of 3 bohr.

We turn now to the case of an anion vacancy in the second layer. In the absence of the oxygen adsorbate, the Mulliken populations indicate (Tables V—VII) that approximately one electron is localized on the vacancy. This number is only an estimate due to the diffuse nature of the O^{2-} basis set, but one could describe the state with some confidence as a singly ionized vacancy with an active species Ni^{1+} on the surface. The qualitative alteration in the Ni configurations is more important than the exact charge, as in Ref. 2. The potentials for adsorbing O, O^-, and O^{2-} are shown in Fig. 6. This is a proper description for Ni on the semi-infinite solid as it is consistent in a local orbitals theory with the insulating character of NiO.[2]

For the neutral adsorption case, there are two distinct competing electron configurations, labeled *A* and *B*. The *A* case shows little change in the electronic distribution from the base of infinite separation. In the *B* case, an electron has transferred from the surface to the adsorbate. The two states are degenerate in the vicinity of 5.2 bohrs. Below the distance of the electron transfer, which alters the nickel ion closer to its preferred 2+ condition, a

TABLE VII. O^{2-} above Ni above second-layer vacancy.

Type	Distance	Energy	Vacancy	Mulliken populations Surface O	Surface Ni	Adsorbed O
A	∞	0.000 00	0.9113	7.9614	9.2433	10.0000
A	8	−0.042 90	0.9985	7.9743	9.1414	9.9627
A	6	−0.047 64	1.0238	7.9808	9.1182	9.9347
A	5	−0.051 09	1.0426	7.9844	9.1255	9.8943
A	4	−0.046 97	1.0415	7.9840	9.1811	9.8416
A	3	+ 0.074 3	1.0229	7.9680	9.3298	9.7751

		Populations on surface Ni by character		
Type	Distance	*s*	*p*	*d*
A	∞	0.4586	0.7679	8.0167
A	8	0.4212	0.7009	8.0193
A	6	0.3910	0.7095	8.0176
A	5	0.3863	0.7208	8.0183
A	4	0.3709	0.7901	8.0201
A	3	0.3724	0.9486	8.0265

TABLE VIII. O_2 above Ni above second-layer vacancy.

Distance	Energy	Vacancy	Mulliken populations Surface O	Surface Ni	Lower O	Higher O	O_2 bond
∞	0	0.9113	7.9614	9.2433	7.8926	7.8926	0.2147
10	−0.001 86	0.9094	7.9615	0.2494	7.8878	7.8927	0.2147
8	−0.007 01	0.8900	7.9622	9.2648	7.8921	7.8899	0.2144
6	−0.015 88	0.8661	7.9635	0.2757	7.9118	7.8790	0.2134
5	−0.019 09	0.8526	7.9633	9.2954	7.9107	7.8756	0.2124
4	−0.017 17	0.8013	7.9561	0.3751	7.9245	7.8641	0.2102

Distance	Populations on surface Ni by character s	p	d
∞	0.4586	0.7679	8.0167
10	0.4650	0.7674	8.0171
8	0.4661	0.7813	8.0172
6	0.4526	0.8075	8.0156
5	0.4538	0.8237	8.0179
4	0.4192	0.9362	8.0197

strong bond is formed, with energy probably greater than 1 eV. In the dynamic situation, the spin barrier should be readily overcome. This is particularly true given the strength of the magnetic interactions in NiO which destroy $\vec{S}$ as a good quantum number. This is a significant effect in an originally neutral system.

In the case of O^-, a charge shift to the adsorbate, if it occurs at all, occurs closer to the surface and is not nearly as pronounced. The point at 3 bohrs has been tentatively identified as belonging to a *B*-type state because of the changes in the Mulliken populations but this is by no means certain. In this region both the O^- and the O curves have an ionized adsorbate; it is the surface nickel whose charge is different. In the case of O^{2-}, no charge transfer is possible to the closed-shell adsorbate, and a broad trough is observed compared with the binding curve determined for the case of the perfect surface.

Of the sites discussed so far, the one which displayed the most interesting features was the second-layer anion vacancy in the case of neutral O adsorption. The site was chosen for an extension of the calculations to the adsorption of O_2, which is a good example in which to examine features of molecular adsorption. The orientation of the molecule normal to the surface was chosen as the simplest and most physically realizable case; it also allows direct comparison to the previous calculation without introducing other complications such as symmetry.

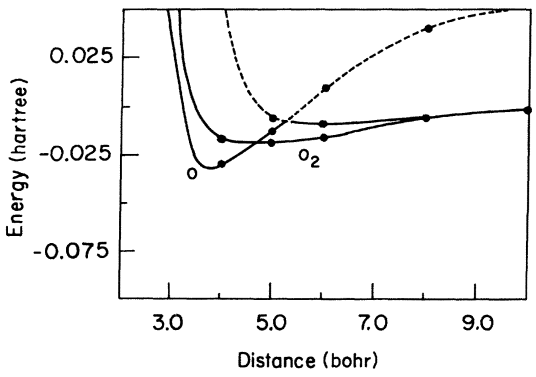

FIG. 7. Binding curve for O_2 above a second-layer anion vacancy with the curve for O repeated for comparison.

The charge transfer to the adsorbate so evident in the atomic adsorption case is completely absent here (Fig. 7 and Table VIII). Evidently the closed-shell nature of O_2 is such that it is energetically unfavorable for the molecule to accept an additional electron from the Ni^{1+}. Such a phenomenon implies that O_2 is not likely to be bound strongly to any surface defect.

Here is a clearcut case where dissociation is encouraged. The bonding for the O atom is considerably stronger than that for the O_2 molecule; it is here probable that a site not too different from this vacancy could liberate enough energy to catalyze the dissociation mechanism in O_2.

The lack of a strong short-range bond is again reflected in the lower half of Table VIII. Although the Ni^{1+} has considerable *s*- and *p*-character charge, there is little variation in this population in a case in which a strong bond is not formed. Again the pattern of *s*- and *p*-electron activity in surface bonding emerges. All population changes in this example are gradual, which matches well the gentle slope of the potential curve as the molecule moves away from the surface.

IV. CONCLUSIONS

Binding curves for potential adsorption sites have been calculated and compared with the perfect surface. Enhanced binding was observed for defect sites, which are shown to be likely locations for the adsorption of oxygen on NiO. This conclusion is consistent with the observed low surface coverage and the variability of binding energies reported experimentally, as discussed in Sec. I.

What are the reasons for enhanced binding? The general answer is that the introduction of the lattice defect

has so disturbed the electronic structure that the adsorption of an oxygen atom can lead to a state in which there are more closed shells. It is usually energetically favorable for the nickel ion to shed its *s* electrons in favor of completing the oxygen 2*p* shell. This is seen in several of the examples presented earlier.

Are defects distributed uniformly through the solid, or is there a higher concentration near the surface, as proposed by Atkinson and Taylor?[13] If we accept the suggestion[6] to count the defects in the first two layers as surface sites, the highest suggested bulk defect concentration[16] of 2×10^{-4} provides only 0.04% surface coverage if we assume defect sites to be solely responsible for the types of adsorption observed by Iwamoto *et al.*[5] Another possibility is that defect sites in deeper layers may somehow contribute to binding up on the surface. At the most, however, a depth of four atomic layers would be available if the surface layer is of the depth reported by Atkinson and Taylor. As this work supports vacancy sites as the chief bonding sites, the conclusion is reached that the density of vacancies is higher near the surface than in the bulk by at least an order of magnitude, in agreement with the observations of Atkinson and Taylor.

Demuth[17] finds that binding to first-period transition-metal atoms involves electrons not from the *d* shell but from the *s* shell. Calculations reported in this work confirm this finding. In cases where we find strong binding, analysis of Mulliken populations over the basis functions reveals the nature of the electrons which are involved.

The data in Table V demonstrate this clearly. Comparing the *A* and *B* states at 5 bohrs, the closest data point to crossing the *s*-electron population on the surface cation is seen to be different by 0.23, the *p* electron by 0.32, and the *d* electron by 0.01. This case may be compared with the O^- and the O^{2-} cases of Tables VI and VII where such strong binding does not occur and is an indication of the inactivity of the *d* shell. For Ni ions the Ar core was replaced by a pseudopotential, as was the He core of the O atoms in the NiO solid and are thus not included in the Mulliken populations.[1,2]

ACKNOWLEDGMENTS

This research was supported in part by the National Science Foundation Materials Research Laboratories Program under Grant No. DMR-80-20250.

---

*Present address: Department of Chemistry, The Johns Hopkins University, Baltimore, MD 21218.

[1]G. T. Surratt and A. B. Kunz, Phys. Rev. B 19, 2352 (1979).
[2]G. G. Wepfer, G. T. Surratt, R. S. Weidman, and A. B. Kunz, Phys. Rev. B 21, 2596 (1980).
[3]G. T. Surratt and A. B. Kunz, Solid State Commun., 23, 555 (1977).
[4]P. C. Gravelle and S. J. Teichner, Adv. Catal. 20, 167 (1969).
[5]M. Iwamoto, Y. Yuoda, M. Egashira, and T. Seiyama, J. Phys. Chem. Solids 80, 1989 (1976).
[6]H. B. Charman and R. M. Dell, J. Phys. Chem. Solids 23, 1567 (1962).
[7]C.Wagner and K. Hauffe, Z. Elektrochem. 44, 172 (1938).
[8]I. Maxim and T. Braun, J. Phys. Chem. Solids 24, 537 (1963).
[9]T. Yamashina, T. Nagamatsuya, and M. Sano, Bull. Chem. Soc. Jpn. 41, 2257 (1968).
[10]B. Lesage, A. M. Huntz, and P. Lacombe, J. Phys. Chem. Solids 42, 705 (1981).
[11]G. J. Koel and P. J. Gellings, Oxid. Met. 5, 185 (1972).
[12]S. Shirasakim, Y. Moriyoshi, and H. Haneda, in Proceedings of the International Symposium on Factors of Densification Sintering Oxide Non-Oxide Ceramics, Japan, 1978, p. 174.
[13]A. Atkinson and R. I. Taylor, Philos. Mag. A 43, 979 (1981).
[14]J. M. Blaisdell and A. B. Kunz, Solid State Commun. 40, 745 (1981).
[15]M. Prutton, J. A. Walker, M. R. Welton-Cook, R. C. Felton, and J. A. Ramsey, Surf. Sci. 89, 95 (1979); M. R. Welton-Cook and M. Prutton, J. Phys. C 13, 3993 (1980).
[16]Yu. D. Tretyakov and R. A. Rapp, Trans. Metall. Soc. AIME 245, 1235 (1969).
[17]J. E. Demuth, Surf. Sci. 65, 369 (1977).